Cascaded optical cavities with two-level atoms: Steady state

J. Gripp, S. L. Mielke, and L. A. Orozco
Physics Department, State University of New York at Stony Brook, Stony Brook, New York 11794-3800
(Received 19 December 1994)

We have experimentally studied the steady-state characteristics of a cascaded quantum-optical system. The conceptually simple apparatus consists of a pair of high finesse cavities traversed by a beam of optically prepared two-level atoms. The output from the first cavity is coupled through a unidirectional device into the second cavity. The experimental results show quantitative agreement with a model that takes into account the geometric factors of the cavity modes and treats the two-level atoms as being purely radiatively broadened.

PACS number(s): 42.50.Fx, 32.80.−t

I. INTRODUCTION

The interaction of a single mode of the electromagnetic field with a collection of two-level atoms forms a canonical system in quantum optics. From the Jaynes-Cummings model [1] to present day cavity quantum electrodynamics (QED) [2] a long and important effort has now produced a system with the attractive feature that a realistic theory can describe an experiment. Refinements in both parts have enhanced the subject and have made it a unique ground for testing new ideas and insights in different areas of physics. It has been particularly fruitful in the areas of QED [3], nonlinear dynamics [4], and statistical mechanics [5]. The apparent simplicity of two-level atoms coupled to a single mode of the electromagnetic field is contrasted with the wealth of phenomena shown by this system. Examples are optical bistability [6, 7], squeezed states [8–10], and antibunched light [11]. The experimental study continues to expand with work such as the two-photon bistability observed by Grangier *et al.* [12] and the experiments with trapped atoms in cavities by Giacobino *et al.* [13]. Casagrande *et al.* [14] have studied the multistability of a system of N two-level Rydberg atoms traversing a single mode of a resonant cavity and they find multistability and instabilities, while Rosenberger and Kim [15] have found in their calculations transit-induced optical multistability. In cavity QED, the work of Brune *et al.* [16] with Rydberg atoms explores ways to detect the state of the electromagnetic field inside a cavity, while Parkins *et al.* [17] have proposed a means of preparing Fock states of the field inside a cavity.

Continuing advances in the theory of open quantum systems [18–20] now permit the study of the influence of higher than second-order correlation functions on the response of driven quantum-optical systems. We are interested in cascaded optical systems. They present a unique environment for understanding the behavior of open quantum systems. The recent works of Gardiner and Parkins [21] and Kochan and Carmichael [22] stress the importance of appropriate coupling between the cascaded parts. Gardiner and Parkins have investigated two-level atoms driven with light of arbitrary statistics [21]. Specifically, they have studied a two-level atom driven by a coupled atom-cavity system. They show a dramatic enhancement of the antibunching of the light emitted by the two-level atom when it is driven by the output of the atom-cavity system. Kochan and Carmichael [22], in their study of single-atom absorption, require a focusing of the excitation light to an area similar to the absorption cross section of the atom in order to have significant effects originating from the cascaded nature of the problem. We have developed a conceptually simple apparatus (see Fig. 1) where we can control the parameters necessary to study the response of a quantum optical system to nonclassical light. It consists of two cascaded atom cavity units, where the output of the first is unidirectionally coupled to the second.

In our apparatus, the properties of the output from the first atom cavity are ideal to drive a second atom cavity. Since the first atom cavity can produce a great variety of nonclassical states of light, the response of this cascaded system offers a means of addressing questions about light with different quantum statistics. As a first step towards this goal, we present here investigations of the steady-state behavior of a cascaded quantum optical system. We have measured the steady-state characteristics of an apparatus that consists of two cascaded single-mode optical cavities traversed by a collimated beam of optically pumped rubidium atoms. The rubidium behaves as a collection of two-level atoms. A coherent source drives the first cavity, the output of which is coupled through a unidirectional device into the second.

In this paper we present our study of the output of the cavities as a function of the system parameters to find regions of bistability. For certain parameters both cavities show bistability in their input-output characteristics. We compare the experimental data with theoretical predictions obtained from a model where each cavity has a

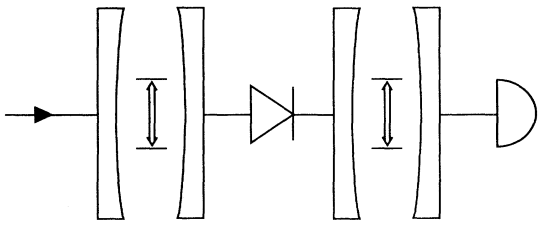

FIG. 1. Schematic idea of the cascaded atom cavities.

single mode of the electromagnetic field interacting with a collection of homogenously broadened two-level atoms. In Sec. II we describe this model. Section III presents the experimental apparatus and procedure in some detail. The results and comparisons with theory are in Sec. IV, while Sec. V contains the conclusions.

II. THEORY

The theoretical model used in the understanding of the cascaded cavities comes directly from the ample literature on optical bistability [6, 23, 24]. Since our system consists of two bistable cavities, we express the state equation in terms of the input to the first cavity and the output of the second one. We take the output from the first cavity as the input to the second cavity while allowing the efficiency of coupling to be less than unity.

The problem of a single cavity has been thoroughly studied theoretically [6]. In the semiclassical approximation, with fields treated classically, a set of Maxwell-Bloch equations describes the model. We make the following assumptions: (i) Only one mode of the electromagnetic field of the cavity interacts with the atoms. (ii) The single pass absorption by the atoms is small. (iii) The reflectivity of the mirrors is high. (iv) In the uniform field limit [6], the absorption by the atoms and the transmission of the mirrors go to zero, while their ratio remains constant and arbitrary. (v) The atoms are allowed to decay only through a radiative process. (vi) The atoms are distributed near the cavity waist within a distance that is small compared to the Rayleigh length in order to neglect the longitudinal variation of the cavity-mode diameter. In addition to these assumptions, we include the standing-wave configuration for the cavity as well as the Gaussian transverse profile of the cavity mode.

Under the appropriate boundary conditions the steady-state solution of the Maxwell-Bloch equations gives the state equation [23, 24]. The state equation relating the input and output intensities for cavity 1 is

$$Y = X[(1 + 2C_1\chi_1)^2 + (\theta_1 - 2C_1\Delta_1\chi_1)^2], \tag{1}$$

where χ_1 has the form

$$\chi_1 = \frac{3}{2X}\ln\left[\frac{1}{2} + \frac{1}{2}\left(1 + \frac{8X}{3(1+\Delta_1^2)}\right)^{1/2}\right]. \tag{2}$$

In Eq. (1), Y is the intracavity intensity in the absence of atoms, normalized to the saturation intensity, and is related to the input intensity by the enhancement factor of the cavity. X is the intracavity intensity in the presence of atoms, normalized to the saturation intensity, and is related to the output intensity by the transmissivity of the exiting mirror:

$$Y = 3\frac{P_{i,1}}{\pi w_{0,1}^2 I_s}\frac{T_{0,1}}{T_{2,1}}, \tag{3}$$

$$X = 3\frac{P_{t,1}}{\pi w_{0,1}^2 I_s}\frac{1}{T_{2,1}}. \tag{4}$$

Here $P_{i,1}$ and $P_{t,1}$ are the incident and transmitted powers of cavity 1, $w_{0,1}$ is the TEM_{00} mode waist of the cavity, and $I_s = \pi hc/3\tau\lambda^3$ is the saturation intensity of the atomic transition, defined as the power per unit area delivered on resonance by one photon of wavelength λ over the atomic absorption cross section every two lifetimes τ. The enhancement factor of the cavity $T_{0,1}/T_{2,1}$ takes into account the presence of other losses in the cavity due to absorption and scattering on the mirrors. These losses give an overall cavity transmission $T_{0,1}$ of less than unity. The transmissivities of the entrance and exit mirrors are $T_{1,1}$ and $T_{2,1}$.

The cavity and atomic detunings are given by θ_j and Δ_j, respectively,

$$\theta_j = \frac{\omega_{c,j} - \omega_0}{\kappa_j}, \tag{5}$$

$$\Delta_j = \frac{\omega_{a,j} - \omega_0}{\gamma_\perp}, \tag{6}$$

where $j = 1$ or 2, identifying the cavity in Eqs. (5) and (6). $\omega_{c,j}$, ω_0, and $\omega_{a,j}$ are the frequencies of the cavity resonance, the excitation source, and the atomic resonance. The detunings are measured in units of the cavity half-width κ_j and the atomic resonance half-width $\gamma_\perp$. Since there is only radiative decay in the model, $2\gamma_\perp = \gamma_\parallel$, with $\gamma_\parallel = \tau^{-1}$, where τ is the radiative lifetime of the atomic transition. The cooperativity parameter C_j is half the ratio of the atomic absorption loss to the round-trip cavity loss. Following Rosenberger *et al.* [23] we define it in terms of measured quantities

$$C_j = \frac{(\alpha_0 l)_j}{2}\left[\frac{T_{0,j}}{T_{1,j}T_{2,j}}\right]^{1/2} \tag{7}$$

or as

$$C_j = \frac{(\alpha_0 l)_j F_j}{2\pi}, \tag{8}$$

where α_0 is the small signal absorption coefficient on resonance, l is the length of the atomic medium, and F is the finesse of the cavity, defined as the ratio of the free spectral range (FSR) to the full width at half maximum (FWHM) of the cavity resonance. The small signal absorption is related to the atomic density ρ by

$$\alpha_0 = \rho\sigma_0, \tag{9}$$

where σ_0 is the on resonance absorption cross section for a two-level atom with transition wavelength λ,

$$\sigma_0 = \frac{3\lambda^2}{2\pi}. \tag{10}$$

Rosenberger *et al.* [23] showed the equivalence of both definitions of C. This in itself provides a test for the consistent measurement of the cavity properties. A further constraint comes from measuring the ratio $R_{0,j}$ of on-resonance reflected power to off-resonance reflected power from the standing-wave cavity and then verifying the relationship

$$\sqrt{R_{0,j}} + \sqrt{T_{0,j}} = 1. \tag{11}$$

There is an important connection between the opera-

tional definition of cooperativity given above and the fundamental coupling constant g_0 from cavity quantum electrodynamics [2]. The cooperativity is the ratio of good coupling between the mode and the atom through the dipole transition to bad coupling to other modes either through spontaneous emission or through escape from the cavity.

In general, for a dipole moment μ connecting the two energy levels of the atom with transition frequency ω in a mode volume V, the coupling constant g_0 is

$$g_0 = \sqrt{\frac{\omega\mu^2}{2\hbar\varepsilon_0 V}}. \tag{12}$$

This coupling constant between one atom and the cavity, also called the single-photon Rabi frequency, represents the reversible internal evolution of the field inside the cavity. For the case of optimal coupling for N purely radiatively broadened two-level atoms, without taking into account the specific geometric and filling factors of the mode, the cooperativity is related to g_0 by

$$C = \frac{g_0^2 N}{\gamma_\parallel \kappa}. \tag{13}$$

The extention of this model to include a second cavity is straightforward. The transfer efficiency η takes the output power exiting cavity 1 and converts it into the input power to cavity 2:

$$P_{i,2} = \eta P_{t,1}. \tag{14}$$

The state equation for the second cavity is

$$W = Z[(1 + 2C_2\chi_2)^2 + (\theta_2 - 2C_2\Delta_2\chi_2)^2], \tag{15}$$

where χ_2 has the form

$$\chi_2 = \frac{3}{2Z}\ln\left[\frac{1}{2} + \frac{1}{2}\left(1 + \frac{8Z}{3(1+\Delta_2^2)}\right)^{1/2}\right]. \tag{16}$$

The input $P_{i,2}$ and transmitted $P_{t,2}$ powers from cavity 2 relate to the dimensionless input W and output Z intensities by

$$W = 3\frac{P_{i,2}}{\pi w_{0,2}^2 I_s}\frac{T_{0,2}}{T_{2,2}}, \tag{17}$$

$$Z = 3\frac{P_{t,2}}{\pi w_{0,2}^2 I_s}\frac{1}{T_{2,2}}. \tag{18}$$

$w_{0,2}$ is the mode waist and I_s is the saturation intensity. The enhancement factor of cavity 2 is $T_{0,2}/T_{2,2}$ and the transmissivity of the exit mirror $T_{2,2}$. With the help of Eqs. (1) and (15) the relationship between the input Y to cavity 1 and the output Z from cavity 2 is established.

III. EXPERIMENT

A. Apparatus

The experimental apparatus (see Fig. 2) consists of three main parts: first, the vacuum system where the collimated atomic beam of rubidium is optically prepared and interacts with the single modes of the two cavities; second, the lasers, optics, and detectors that produce, control, and measure the light that interacts with the atoms and the cavities; and third, the two optical cavities themselves where the interaction between the atoms and a single mode of the electromagnetic field takes place.

The vacuum system is pumped by an oil diffusion pump and consists of a stainless-steel chamber and a series of commercially available components. The pressure typically ranges from 10^{-5} Pa to 10^{-4} Pa. The effusive oven has a single aperture of 1 mm width and 5 mm height. When resistively heated, it produces an atomic beam in the chamber. Of the two isotopes available, all the work reported here has been done with the more abundant ^{85}Rb. 47 cm downstream from the oven aperture the atoms encounter the first interaction region. For each of the interaction regions a set of three orthogonal coils nulls the magnetic field of the earth and other stray fields from the laboratory to better than 10^{-6} T while providing a field of 10^{-4} T parallel to the cavity axis. Before the atomic beam enters the first cavity, it is optically prepumped. A 0.7-mm entrance aperture fixed to the first optical cavity collimates the beam. Immediately downstream from the first cavity, a weak laser beam with the appropriate polarization monitors the signal absorption $\alpha_0 l$. The atomic beam then travels 26 cm to the second interaction region. Before entering the cavity it is optically pumped, this time with two lasers. A 0.2-mm aperture collimates the beam. As the atoms exit the second cavity they encounter the second monitor beam, this time an intense one used to measure their fluorescence in a direction perpendicular to that of the laser and that of the atomic beam. The atomic beam is then dumped into a cold surface.

On resonance we can reach an absorption equivalent to an $\alpha_0 l > 0.20$, permitting us to examine ample regions of the cooperativity parameter in the first interaction region, while fulfilling the conditions for the uniform field limit of the model [6]. There is no Doppler pedestal on our atomic beam absorption or fluorescence. The residual Doppler broadening on the beam (0.8 MHz FWHM) broadens the radiative linewidth from 6.2 to 6.4 MHz.

The main excitation source for the experiment is a titanium sapphire laser operating at 780 nm pumped by a 5-W argon ion laser. We actively stabilize the laser by deriving an error signal from FM saturation spectroscopy [25] on a rubidium cell. The resulting linewidth of the laser is less than 300 kHz. The main laser is divided into the signal beam and the service beams: optical pumping of the atomic beam and monitoring of the absorption. Since there are two cavities, there are two regions where the atoms are pumped. We circularly polarize the laser beams using a polarizer followed by a quarter-wave plate. This process prepares the rubidium atoms in the $5\,^2S_{1/2}$, $F = 3$, m_F=3 state from which they can reach only the $5\,^2P_{3/2}$, $F = 4$, m_F=4 state via excitation by light of the same circular polarization, producing an effective two-level atom. The second source is a Sharp LT024 diode laser, frequency narrowed using strong feedback from a grating [26]. We actively lock this laser close to the $F = 2 \rightarrow F' = 3$ atomic transition using saturation

spectroscopy in another rubidium cell. This laser acts as the repumper.

The signal beam is intensity modulated using a liquid crystal variable phase retarder between polarizers and then cicularly polarized and mode matched into the first optical cavity (see Fig. 2). Part of the incoming signal goes to a calibrated photodiode to give a measurement of the input intensity of the cavity. The signal beam has 12-MHz FM sidebands used for locking the cavity on reflection [25]. The reflected beam is picked off out of the polarizer that acts as an optical diode in combination with the quarter-wave plate. The output of the first cavity is then directed to the second cavity. A beam splitter sends a small fraction towards a photomultiplier to measure the output from cavity 1. A quarter-wave plate converts the polarization of the light back to linear. The light then encounters a second optical diode formed by a polarizer and a quarter-wave plate. As it exits the cavity it is focused onto a photomultiplier tube for detection of the transmitted intensity from the cascaded system.

The cavities consist of a central body made of stainless steel. Four holes enable the atomic beam to pass through in one direction, while the fluorescence emitted by the atoms as they interact with the cavity mode can escape in the direction perpendicular to the atomic beam and the mode. The mirrors are glued to piezoelectric transducers (PZTs), which themselves are glued to stainless-steel inserts. The mirrors have a 1.27 cm diameter and are separated by 1 mm. The frequency separation between transverse modes for the cavities used in these experiments is larger than 6 GHz, so the atoms interact only with the TEM_{00} mode of the electromagnetic field of the cavities. For some of the results presented in Sec. IV, cavity 1 had a mirror separation of 3 mm.

B. Procedure

Before closing the vacuum system, we align a travelling telescope to sight along its central axis. The oven is positioned on a translating stage movable from outside the chamber. Its aperture is aligned with the centered cross hairs of the telescope. We then insert the holding body of cavity 1 and align the aperture to coincide with

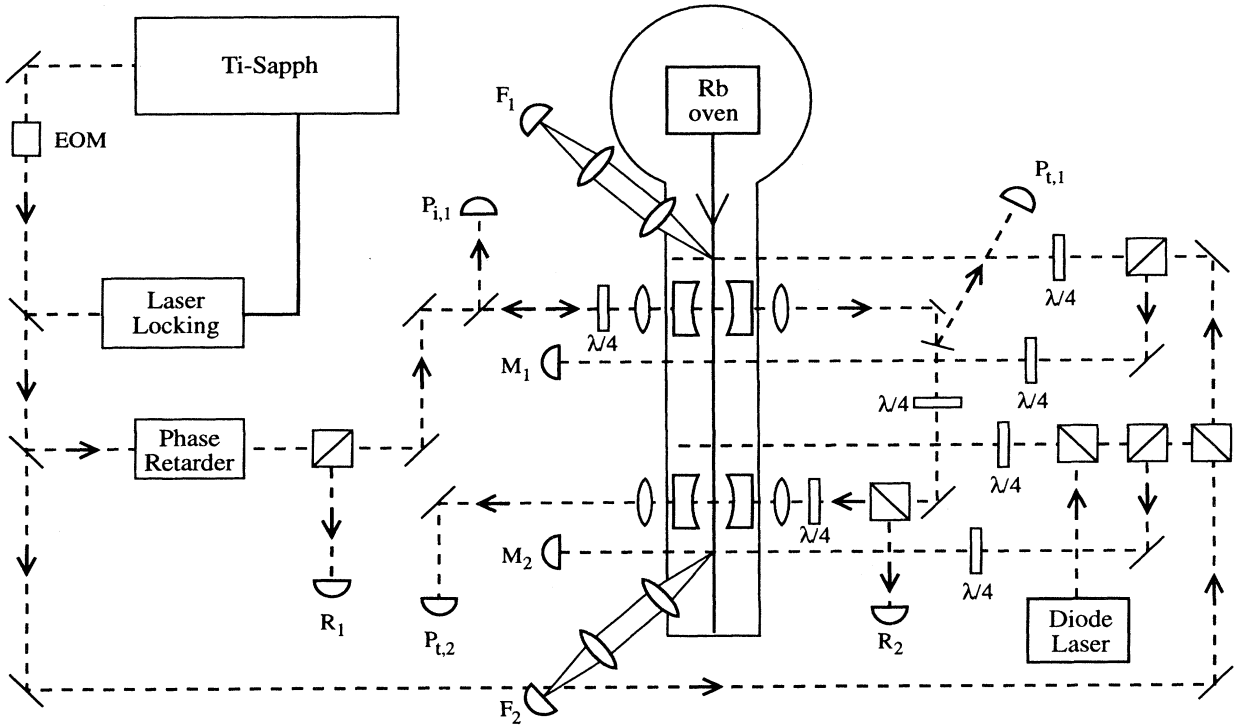

FIG. 2. Experimental setup. In each of the two interaction regions, the atomic rubidium beam encounters consecutively three laser beams, each perpendicular to the atomic beam. In the region closer to the rubidium oven, the first laser beam optically prepumps the atoms into the two-level transition of the D_2 line of ^{85}Rb. Its fluorescence is collected onto the photomultiplier tube F_1. The second light beam is the signal beam. It is intensity controlled by the phase retarder, circularly polarized by a polarizing beam splitter and a quarter-wave plate ($\lambda/4$), which also serve as an optical diode, and then mode matched into cavity 1. The third beam is a weak monitor beam to measure the small-signal absorption on M_1. R_1 detects the reflected power from cavity 1 and serves to lock the cavity on resonance with the help of FM sidebands generated by the electro-optical modulator (EOM). The input power to cavity 1 is measured with the photodiode $P_{i,1}$. A small fraction of the transmitted light is directed onto the photomultiplier $P_{t,1}$. The output of the first cavity is circularly polarized and mode matched before entering the second cavity. In the second interaction region two coincident lasers pump the atoms into the appropriate hyperfine ground state. The photomultiplier $P_{t,2}$ collects the output from cavity 2, while the photodetector R_2 positioned at the optical diode measures the reflection from cavity 2. The transmitted light of the monitor for cavity 2 goes into the photodiode M_2, while its fluorescence is collected onto the photomultiplier F_2. The figure is not to scale.

the oven aperture. Finally, the holding body of cavity 2 is placed and aligned with the apertures of cavity 1 and the oven. If misalignment happens during pump down, some correction is possible with the external controls of the oven position.

Once the chamber is under vacuum and the oven reaches a temperature of 150 °C, we observe the atomic resonance signals in fluorescence and in absorption. We examine the monitor of cavity 2 to maximize the signal of the atomic beam by translating the oven in the horizontal plane. In most experimental runs we have found that the initial position was indeed optimal, which gives us confidence in the alignment procedure.

We make the service beams perpendicular to the atomic beam. The size of the laser beams is large enough to pump and sample the atoms interacting with the much smaller signal beam inside the resonators. We have previously checked that the absorption measured by the monitor beam is the same as in the signal beam located 1.5 cm upstream. The optical pumping and the monitor resonances coincide with the appropriate resonance from a saturation spectroscopy setup to within 0.5 MHz, which in the geometry of the experiment translates into less than 1.3 mrad of misalignment between the atomic beam and the service beams.

With the service beams aligned, we proceed to calibrate the two absorption $(\alpha_0 l)_j$ signals. We first measure the relative sizes of both signals using very weak laser beams: less than 1% of the saturation intensity. The ratio of absorption in cavity 1 to that in cavity 2 is consistent with a calculation for the atomic beam intensity that takes into account the geometric factors and the presence of the repumping laser for the second interaction region. However, to ensure a correct measurement, we also calibrate the fluorescence from the monitor beam of cavity 2 at a high intensity against the small signal absorption $(\alpha_0 l)_1$. This permits us to measure the number of atoms in both cavities at small Rb beam intensities.

We measure the properties of both cavities and their mode matching efficiency at the begining and at the end of the experiment. The properties of the five cavities used for these experiments are specified in Table I. We record the on-resonance empty cavity transmission T_0 as well as the empty cavity reflection R_0 and we check for consistency using Eq. (11). The finesse, measured by scanning the cavity length, gives us another check to verify that the cavity properties are well understood. We have measured the transmissivity of the mirrors on various occasions and have seen no change. In Table I we only report the exit transmissivity since we have found that $T_{1,j} \approx T_{2,j}$ in all cases. We have seen, however, a degradation on the finesse after repeated exposure to the traversing rubidium beam. The finesse is recovered after cleaning the mirrors with standard techniques.

TABLE I. Cavity and atom-cavity properties for the experiments reported.

Cavity	FSR (GHz)	κ (MHz)	T_2 (ppm)	g_0 (MHz)	w_0 (τ)
A	50	12.0	100	0.95	23
B	150	63.0	100	3.9	10
C	150	21.0	100	3.9	10
D	150	1.5	13	2.6	15
E	150	1.0	13	2.6	15

Once the calibrations are performed, we turn the oven temperature up slowly while we record the input-output characteristics from the first cavity. The wave form driving the variable phase modulator permits us to remain at the highest transmission point for 1 s and then ramp the intensity down and up in 4 ms. While the first cavity is locked, we scan the cavity length of the second cavity near resonance and look for changes in the transmission while the atoms are present or absent.

Our operational definition of atomic on-resonance excitation ($\Delta = 0$) for cavity 1 is the absence of dependence of the bistability switching points Y_1 and Y_2 on the sign of the cavity detuning θ. When this condition is fulfilled, the signals derived from the service beams (optical pumping fluorescence and monitor absorption) are also on resonance.

We calibrate, against a National Institute of Standards and Technology traceable photodetector, all the photodiodes and photomultiplier tubes used to detect the input and output powers of both cavities. Then we can extract the normalized intensities X, Y, Z, and W that permit us an absolute comparison with theory.

IV. RESULTS

We start by studying the behavior of the first cavity. The theoretical predictions are based on the model presented in Sec. II. Further refinements of the model, particularly the treatment of inhomogeneous or transit time broadening [23], do not significantly change the predictions, given the particular parameters of the experiment. Table I contains the transit time across the diameter of the TEM_{00} mode in units of the radiative lifetime of the atomic transition $\tau = 25.5$ ns. The atom-cavity coupling constant g_0 for the different combinations of length and mirrors used is also given in Table I.

We have observed optical bistability in the output transmission of the first cavity. The hysteresis devel-

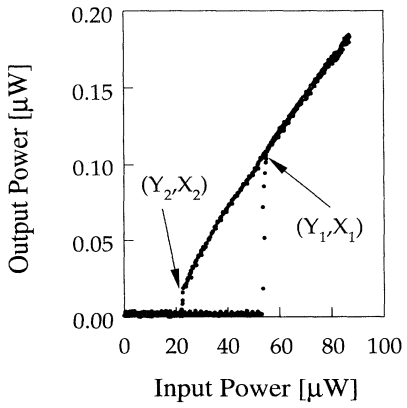

FIG. 3. Optical bistability observed in the transmitted power vs incident power for cavity A ($C \approx 33$).

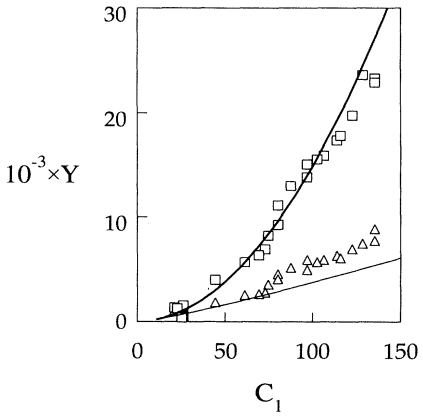

FIG. 4. Normalized input switching intensities for cavity A as a function of cooperativity C_1. The squares (□) correspond to the switch up normalized input intensity Y_1 and the triangles (△) correspond to the switch down normalized input intensity Y_2 of Fig. 3. The curves are the predictions from the theory.

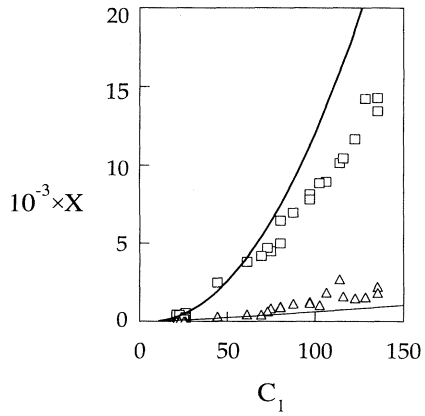

FIG. 5. Normalized output switching intensities for cavity A as a function of cooperativity C_1. The squares (□) correspond to the switch up normalized output intensity X_1 and the triangles (△) correspond to the switch down normalized output intensity X_2 of Fig. 3. The curves are the predictions from the theory.

ops as C_1 is increased by raising the oven temperature to increase the atomic density. Figure 3 shows an input-output trace with a well developed hysteresis when we used cavity A.

The first step in the quantitative understanding of the system is the measurement (from a series of traces similar to Fig. 3) of the input Y_1 and Y_2 switching intensities of bistable curves as the atomic density changes. The results using cavity A are in Fig. 4. The overall uncertainty in the horizontal axis is 30%, coming from the cavity properties and the calibration of the absorption of the atomic beams. The vertical axis has an overall uncertainty of 15%, coming from the calibration of the photodetectors and the self-consistency of the properties of the cavity. We have explored values of the cooperativity parameter 13 times larger than the critical value necessary for bistability. The theoretical curves have no adjustable parameters and the agreement we see in the absolute values is good.

At the same time that we record the input intensity we also measure the output intensity. Figure 5 presents the data for the normalized transmitted intesity. We measure the intensity the cavity reaches as soon as it switches to the upper branch X_1 and the intensity jump when it switches to the lower branch X_2. The overall uncertainty in the horizontal axis is 30% and the vertical axis is 15%. Again the agreement is good.

With the first cavity well understood, we proceed to measure the properties of the cascaded system formed cavity C followed by cavity D in positions 1 and 2, respectively. The transfer efficiency η [Eq. (14)] from the output of cavity 1 to the input mirror of cavity 2 is greater than 80%. We scan the second cavity and observe the influence of the resonantly driven atoms ($\Delta_1 \approx \Delta_2 \approx 0$) on its transmission. Figure 6 shows two traces of the cavity transmission as we scan the mirror spacing by changing the voltage to a PZT. The input Y to cavity 1 is held constant while we scan across the resonance of cavity 2 in 1.5 ms. The thin trace shows the empty cavity transmission. The sidebands used for locking cavity 1 are clearly visible and serve as 12-MHz markers. The thick trace shows the same cavity transmission in the presence of atoms. As seen in the inset, cavity 1 is bistable. The experimental conditions for the cascaded system are $C_1 = 45$, $C_2 = 19$, $Y = 12\,000$, $X = 11\,000$, and $W = 680$ with 20% uncertainties. There is a sharp turn up and down of the cavity transmission as well as a lower peak output intensity. Figure 7 shows the prediction for the model with the parameters from Fig. 6. In the experiment we observe an earlier turn down in the cavity that we attribute to the presence of noise. The turn down detuning of the transition was not as stable as the turn up detuning. Simple

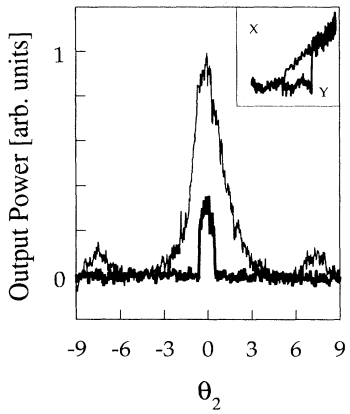

FIG. 6. Transmitted power out of the cascaded system (cavities C and D) as a function of cavity 2 detuning θ_2, with $\Delta_1 \approx \Delta_2 \approx 0$ in the presence (thick trace) and absence (thin trace) of atoms. θ_2 is measured in half-widths at half maximum of the cavity resonance. The first bistable cavity (see inset) is locked on a high transmission state ($C_1 = 45$, $Y = 12\,000$, $X = 11\,000$) while the resonance of cavity 2 is scanned in 1.5 ms ($C_2 = 19$, $W = 680$). The sign of θ was not detemined experimentally. The uncertainties in the normalized intensities and cooperativities are 20%.

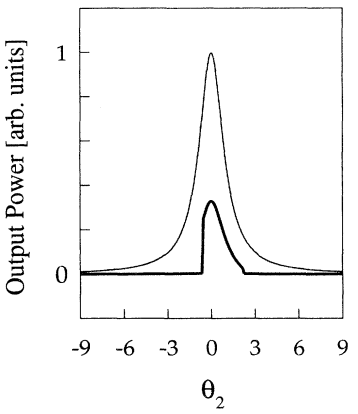

FIG. 7. Calculated transmitted power out of the cascaded system as a function of cavity 2 detuning θ_2 for the experimental conditions of Fig. 6. θ_2 is measured in half-widths at half maximum of the cavity resonance. ($C_1 = 45$, $C_2 = 19$, $\Delta_1 = \Delta_2 = 0$, $Y = 12\,000$, $X = 11\,000$, $W = 680$.) The thin trace is in the absence atoms and the thick trace is in the presence of atoms.

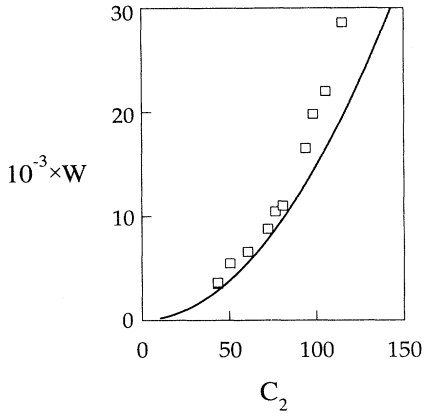

FIG. 8. Characterization of the cascaded system formed by cavities B and E. The squares (□) show the normalized input intensity W necessary for switching into the high transmission state as a function of cooperativity C_2. The first cavity was also bistable. The curve is the prediction from theory. The overall uncertainties for the vertical axis and for the horizontal axis are 23% and 18%.

modeling of amplitude noise in the input field showed a stronger effect in the turn down value of θ_2, which is consistent with our observations. The ratio of output intensities as well as the turn up value for the cavity detuning are very close to the theoretical prediction. The atoms were excited on resonance.

Finally, Fig. 8 shows the normalized input power W as a function of cooperativity C_2 at the switching point when the cavity goes into transmission mode. We obtained the data points by reducing the input power to cavity 1 (B in Table I) until nothing got transmitted out of cavity 2 (E in Table I), while cavity 2 was scanned through resonance. The comparison with theory has no adjustable parameters and although there seems to be a systematic error in our calibration of the cooperativity, the agreement is good and shows the correct functional form for the evolution of the switching point as the cooperativity increases. The overall uncertainty in the horizontal axis is 18%, coming mainly from the cavity properties, while the vertical axis has an uncertainty of 23%, with $T_{0,2}$ contributing the most.

V. CONCLUSION

We have characterized the steady state of a cascaded quantum-optical system. The apparatus consists of a well collimated beam of two-level rubidium atoms (nearly Doppler-free) interacting consecutively with a single transverse mode of two high finesse cavities. The comparison with the theoretical model presented in Sec. II gives us confidence that we understand all the macroscopic parameters of the system. Although the theoretical model treats the fields classically, the absolute agreement we obtain within our quoted uncertainties represents the basis for extentions into the quantum regime. The importance of a good understanding of the steady state for photon counting experiments in cavity QCD has been stated by the work of Thompson [27]. g_0, the fundamental coupling constant of cavity QED, is directly related to the cooperativity parameter C of our model. We have measured C using the steady-state characteristics and we expect to optimize the conditions of the apparatus to study the response of a quantum-optical system to nonclassical light.

We observed bistability in both cavities with input and output switching powers that agree with quantitative predictions from the model. Our uncertanties in the measurements come mainly from the lack of consistency in the properties of the high finesse cavities. We have improved our understanding of the properties of the cavities from the original cavity A (see Table I) to the present cavities. All quantities are measured in absolute terms and we compare them without any adjustable parameter to the model. We have repeated the experimental measurements, obtaining similar results to those presented here.

The system is very well suited for the study of the response of a quantum-optical system to nonclassical light in the spirit of the recent work of Gardiner and Parkins [21] and Kochan and Carmichael [22]. The good agreement obtained with the model serves for extensions into the quantum regime.

The nonlinear dynamics of the system remain to be explored. We have already observed the single-mode instability [28] of optical bistability with the first cavity. The enhancement of the parameter space in the cascaded system will probably present complex dynamical behavior.

ACKNOWLEDGMENTS

We wish to thank H. J. Carmichael for helpful discussions. The support and interest in this research of H. Metcalf is gratefully acknowledged. This work was initiated with financial support from the State University of New York at Stony Brook, generous equipment loans from Grumman Corporate Research Center, and continuing support in part by the National Science Foundation.

[1] E. T. Jaynes and F. W. Cummings, IEEE J. Quantum Electron. **51**, 89 (1963); M. Tavis and F. W. Cummings, Phys. Rev. **170**, 379 (1968).

[2] See, for example, *Cavity Quantum Electrodynamics*, edited by P. R. Berman (Academic, San Diego, 1994).

[3] See, for example, P. L. Knight and L. Allen, *Concepts of Quantum Optics* (Pergamon, Oxford, 1983).

[4] J. Opt. Soc. Am. B **2** (1) (1985), special issue on instabilities in active optical media, edited by Neal B. Abraham, Luigi A. Lugiato, and Lorenzo M. Narducci; *Optical Instabilities*, edited by R. W. Boyd, M. G. Raymer, and L. M. Narducci (Cambridge University Press, New York, 1986); *Instabilities and Chaos in Quantum Optics II*, edited by N. B. Abraham, F. T. Arecchi, and L. A. Lugiato (Plenum, New York, 1988).

[5] C. W. Gardiner, *Quantum Noise* (Springer-Verlag, Berlin, 1991).

[6] L. A. Lugiato, in *Progress in Optics*, edited by E. Wolf (North-Holland, Amsterdam, 1984), Vol. XXI, p. 69.

[7] H. M. Gibbs, *Optical Bistability: Controlling Light with Light* (Academic, Orlando, 1985).

[8] M. G. Raizen, L. A. Orozco, Min Xiao, T. L. Boyd, and H. J. Kimble, Phys. Rev. Lett. **59**, 198 (1987). L. A. Orozco, M. G. Raizen, Min Xiao, R. J. Brecha, and H. J. Kimble, J. Opt. Soc. Am. B **4**, 1490 (1987).

[9] L. A. Lugiato and G. Strini, Opt. Commun. **41**, 67 (1982).

[10] M. D. Reid and D. F. Walls, Phys. Rev. A **32**, 396 (1985); **34**, 4929 (1986).

[11] G. Rempe, R. J. Thompson, R. J. Brecha, W. D. Lee, and H. J. Kimble, Phys. Rev. Lett. **67**, 1727 (1991); R. J. Thompson, G. Rempe, and H. J. Kimble, *ibid.* **68**, 1132 (1992).

[12] P. Grangier, J. F. Roch, J. Roger, L. A. Lugiato, E. M. Pessina, G. Scandroglio, and P. Galatola, Phys. Rev. A **46**, 2735 (1992).

[13] E. Giacobino, J. M. Courty, C. Fabre, L. Hilco, and A. Lambrecht, in *Laser Spectroscopy*, edited by Louis Bloomfield, Thomas Gallagher, and Daniel Larson, AIP Conf. Proc. No. 290 (AIP, New York, 1993), p. 349; L. Hilico, C. Fabre, and E. Giacobino, Europhys. Lett. **18**, 685 (1992).

[14] F. Casagrande, L. A. Lugiato, W. Lange, and H. Walther, Phys. Rev. A **48**, 790 (1993).

[15] A. T. Rosenberger and Jeong-Mee Kim, Opt. Commun. **101**, 403 (1993).

[16] M. Brune, P. Nussenzveig, F. Schmidt-Kaler, F. Bernardot, A. Maali, J. M. Raimond, and S. Haroche, Phys. Rev. Lett. **72**, 3339 (1994); L. Davidovich, N. Zagury, M. Brune, J. M. Raimond, and S. Haroche, Phys. Rev. A **50**, R895 (1994).

[17] A. S. Parkins, P. Marte, P. Zoller, and H. J. Kimble Phys. Rev. Lett. **71**, 3095 (1994).

[18] H. J. Carmichael, Phys. Rev. Lett. **70**, 2273 (1993).

[19] C. W. Gardiner, Phys. Rev. Lett. **70**, 2269 (1993).

[20] M. I. Kolobov and I. V. Sokolov, Opt. Spectrosc. **62**, 69 (1987).

[21] C. W. Gardiner and A. S. Parkins, Phys. Rev. A **50**, 1792 (1994).

[22] P. Kochan and H. J. Carmichael, Phys. Rev. A **50**, 1700, (1994); Zh. Eksp. Teor. Fiz. **102**, 472 (1992) [Sov. Phys. JETP **75**, 250 (1992)].

[23] A. T. Rosenberger, L. A. Orozco, H. J. Kimble, and P. D. Drummond, Phys. Rev. A **43**, 6284 (1991).

[24] P. D. Drummond, IEEE J. Quantum Electron. **QE-17**, 301 (1981).

[25] R. W. P. Drever, J. L. Hall, F. V. Kowaski, J. Hough, G. M. Ford, A. J. Munley, and H. Ward, Appl. Phys. B **31**, 97 (1983); J. L. Hall, L. Hollberg, T. Baer, and H. G. Robinson, Appl. Phys. Lett. **39**, 680 (1981).

[26] C. E. Wieman and L. Hollberg, Rev. Sci. Instrum. **62**, 1 (1991).

[27] R. J. Thompson, Ph. D. dissertation, University of Texas at Austin, 1994 (unpublished).

[28] L. A. Orozco, H. J. Kimble, A. T. Rosenberger, L. A. Lugiato, M. L. Asquini, M. Brambilla, and L. M. Narducci, Phys. Rev. A **39**, 1235 (1989).